RESEARCH ARTICLE

Rare earth element mobility in halogenated aqueous fluids in the humite-marbles of Ambasamudram, Kerala Khondalite Belt, Indi

A. P. Pradeepkumar and R. Krishnanath

Department of Geology, University of Kerala, Trivandrum 695 581, India

The trace and rare earth elements (REEs) in geochemical systems, both within the earth and on its surface, provide a tool to model the effect of fluids on geological materials. In this study we show that Ca and P have a major role in concentrating REEs in the geological materials. Zr, Ti and rare earth elements have been found to be mobile in aqueous halogenated fluids at Ambasamudram in Tamil Nadu. Large volumes of aqueous fluids have been derived from external sources coinciding with the retrogression of the high-grade marbles in the area.

THE study of the trace and rare earth element (REE) content and their mobility in rocks, especially under the influence of aqueous solutions with high HF concentration, has recently aquired strategic importance. Elements like Ti, Th, U and Zr, previously thought to be immobile have been shown to be mobile[1–4], thus seriously questioning the viability of using many geological materials, especially zirconolite, as repositories for high level waste[1,2]. In this context the marbles and surrounding metapelites and granites of Ambasamudram offer excellent sites for the study of REE mobility in halogenated aqueous fluids.

Geological setting

Assemblages consisting of calcite + dolomite + humite + spinel are abundant in the impure dolomitic marbles of Ambasamudram. A unique co-existing assemblage of humite + chondrodite + spinel + magnesian calcite has been reported from the area[5]. These assemblages are typical of the high grade conditions. However, there are pockets and bands of retrograded assemblages of amphibolite and upper greenschist facies in the area[6]. The assemblages in general are quartz-free.

The mineral assemblages representative of the high grade and retrograde conditions are the following:

Granulite facies, spinel-free assemblages ($P_f << P_s$)

(A) Fo + Cal + Dol
(B) Fo + Cal + Dol + Di [retrograded from (A)]

Granulite facies, spinel-free assemblages (P_f

(C) Fo + Chu + Dol + Cal
(D) Fo + Chn + Dol + Cal
(E) Fo + Tr + Di + Cal
(F) Fo + Tr + Dol + Cal
(F1) Fo + Di + Tr + Dol + Cal

Granulite facies, spinel-bearing assemblages

(G) Fo + Spl + Di + Cal + Dol
(H) Fo + Spl + Cal + Dol
(I) Fo + Spl + Chl + Dol + Cal [retro (H)]
(J) Fo + Chl + Dol + Cal [retrogradec
(K) Tr + Chu + Dol + Cal
(L) Fo + Chl + Spl + Tr + Cal

Amphibolite–upper greenschist facies, ret semblages ($P_f = P_s$)

(M) Tr + Dol + Cal
(N) Tlc + Tr + Dol + Cal [retrograded
(O) Tlc + Cal + Dol [retrograded from

[Abbreviations: Fo: forsterite; Chu: clinoh chondrodite; Dol: dolomite; Cal: calcite; T Di: diopside; Spl: spinel; Chl: chlorite; Tlc:

The area falls within the Kerala Kho (KKB), and is comprised in the SE part of ovil Shear Zone (ASZ), a major Neoproteroz trending ductile shear zone with a sinistr displacement[7] (Figure 1). This shear zone l attention and is thought to extend into Ma the Bongolava–Ranotsara Shear Zone[8], int as the Aswa Shear Zone[9] and also into Lanka[10]. NW–SE trending linear bands bearing marbles and calc-silicates are inter- quartzites. Intense shear effects are evident cataclasites and pseudotachylites occur he folds, refolded isoclinal and plunging sy antiformal folds are common, especia

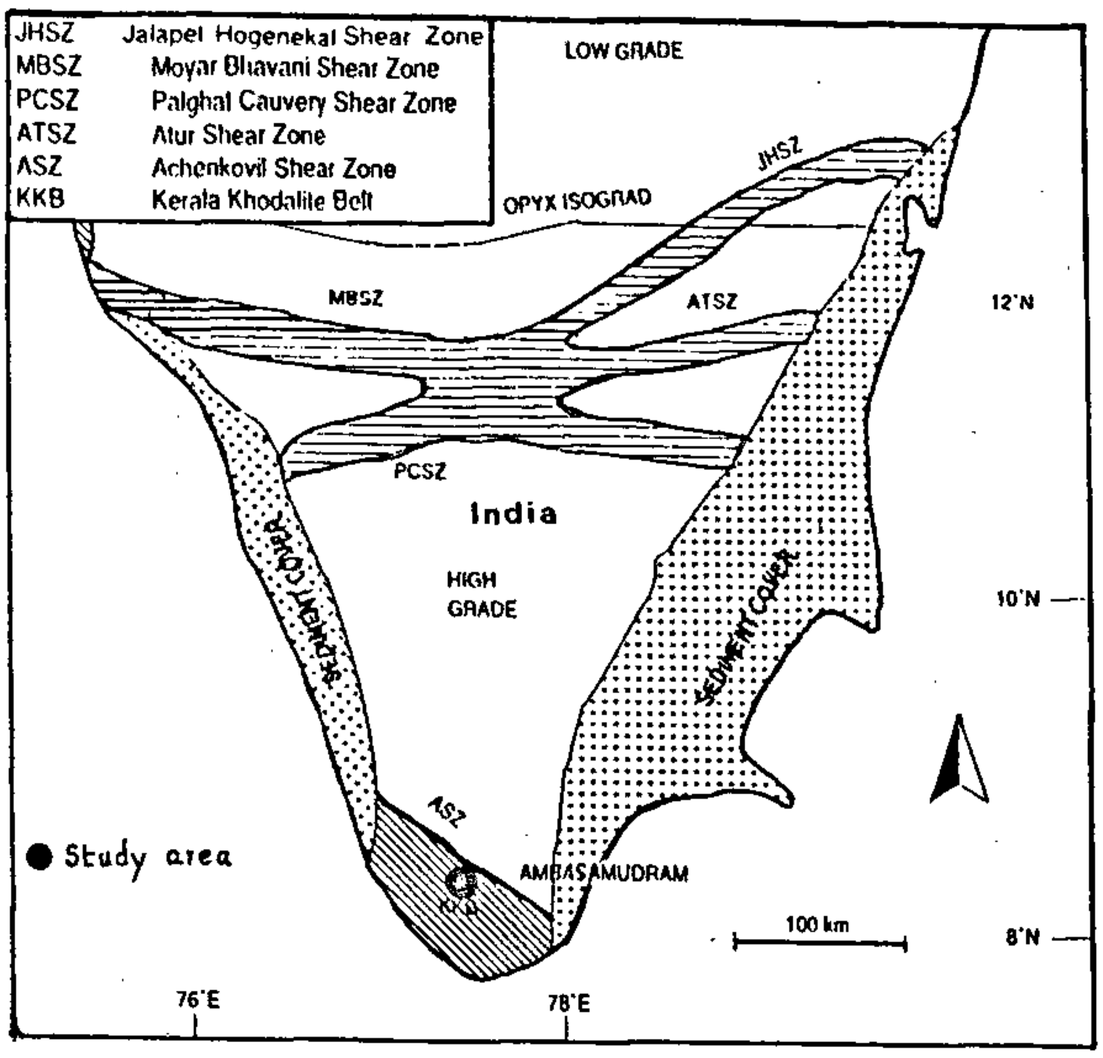

Figure 1. Location of the study area and the shear zones that traverse South India.

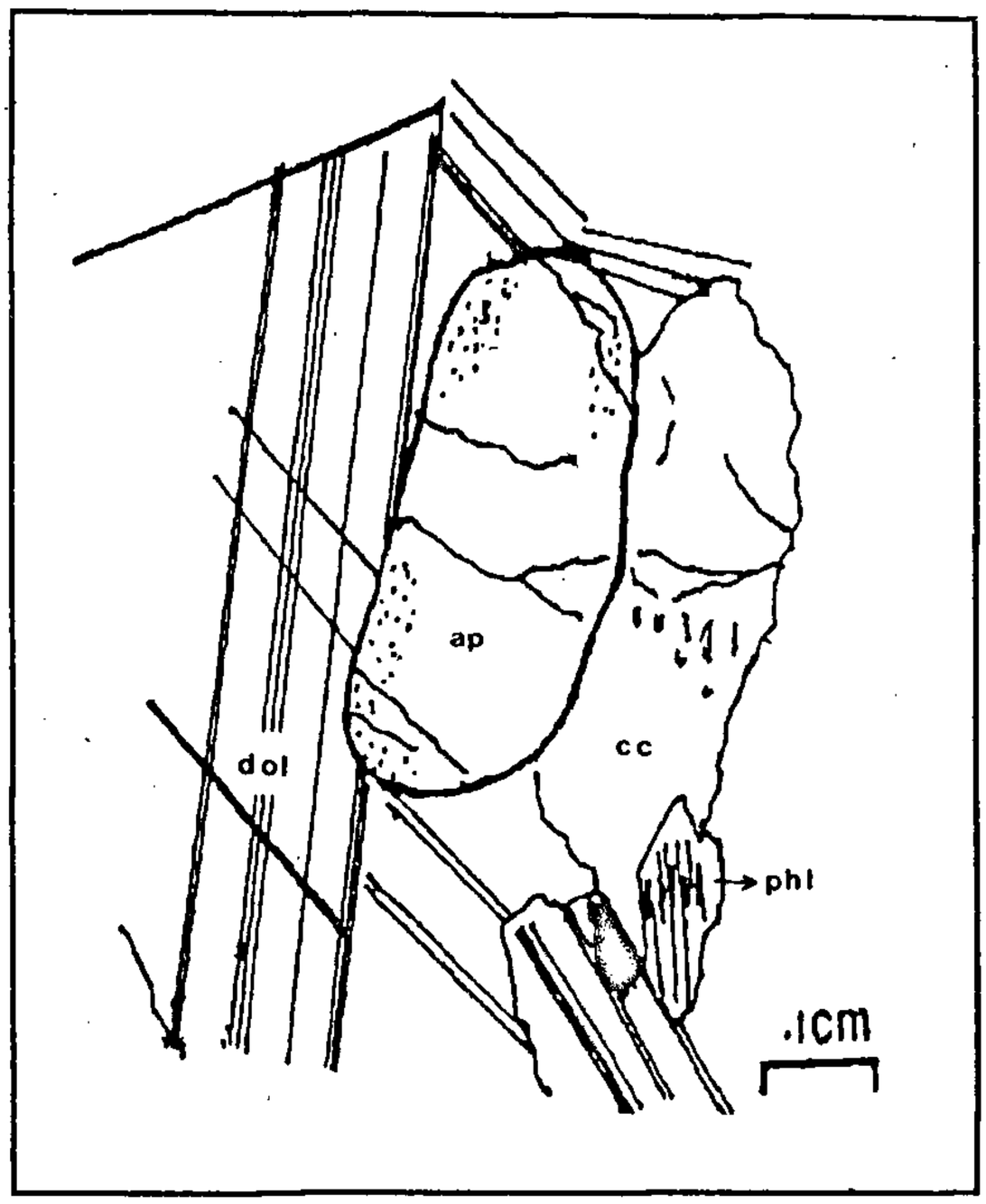

Figure 2. Anhedral apatite (ap), with calcite (cc), dolomite (dol) and phlogopite (phl).

calc-silicates. Large caught up patches of country rocks are preserved unscathed in the mylonites. Diopside, wollastonite and calcite aggregates are flattened and a stretching lineation is defined in the NW–SE direction.

The other rock types include granitoids/granitic gneisses, quartzo-feldspathic sillimanite gneisses and charnockites.

Petrography

Granoblastic textures are observed in the medium to coarse grained calcite–dolomite matrix in the marbles. The mineral phases identified are calcite, dolomite, spinel, chlorite, humites, forsterite, diopside, phlogopite, talc, tremolite and subordinate amounts of apatite (Figure 2), graphite, pyrite, chalcopyrite, magnetite, rutile, ilmenite and zircon. Textural evidence for forsterite and humites getting replaced by diopside and tremolite[11] and the tremolites by talc and carbonates attest to the retrogressive effects. The humites and relict forsterites represent the granulite facies and the other hydrous minerals like tremolite and talc represent later development in amphibolite–upper greenschist facies conditions.

The typical reactions during the granulite facies metamorphism and retrograde metamorphism are:

Forsterite-forming reactions (Figure 3)

$$1Di + 3Dol = 2Fo + 4Cal + 2CO_2 \quad (10)\ [\text{Assemblage A, B}]$$

$$3Tr + 5Cal = 11Di + 2Fo + 5CO_2 + 3H_2O \quad (8)\ [\text{Assemblage E}]$$

$$1Tr + 11Dol = 8Fo + 13Cal + 9CO_2 + 1H_2O \quad (7)\ [\text{Assemblage F}]$$

$$1Chl + 2Dol = 3Fo + 2Cal + Spl + 2CO_2 + 4H_2O \quad (9)\ [\text{Assemblage H, I, J}]$$

Other reactions in the high grade

$$4Fo + Dol + H_2O = Chu + Cal + CO_2 \quad (11)\ [\text{Assemblage C}]$$

$$2Fo + Dol + H_2O = Chn + Cal + CO_2 \quad (12)\ [\text{Assemblage D}]$$

$$3Chl + 2Cal = 5Fo + 2Di + 3Spl + 2CO_2 + 12H_2O \quad (13)\ [\text{Assemblage G}]$$

$$11Chl + 4Cal = 17Fo + 2Tr + 11Spl + 4CO_2 + 42H_2O \quad (14)\ [\text{Assemblage L}]$$

$$Tr + 13Dol + H_2O = 2Chu + 15Cal + 11CO_2 \quad (15)\ [\text{Assemblage K}]$$

Retrograde reaction in amphibolite–upper greenschist facies

$$1Tr + 1Dol + 1CO_2 + 1H_2O = 2Tlc + 3Cal \quad (3)\ [\text{Assemblage M, N, O}]$$

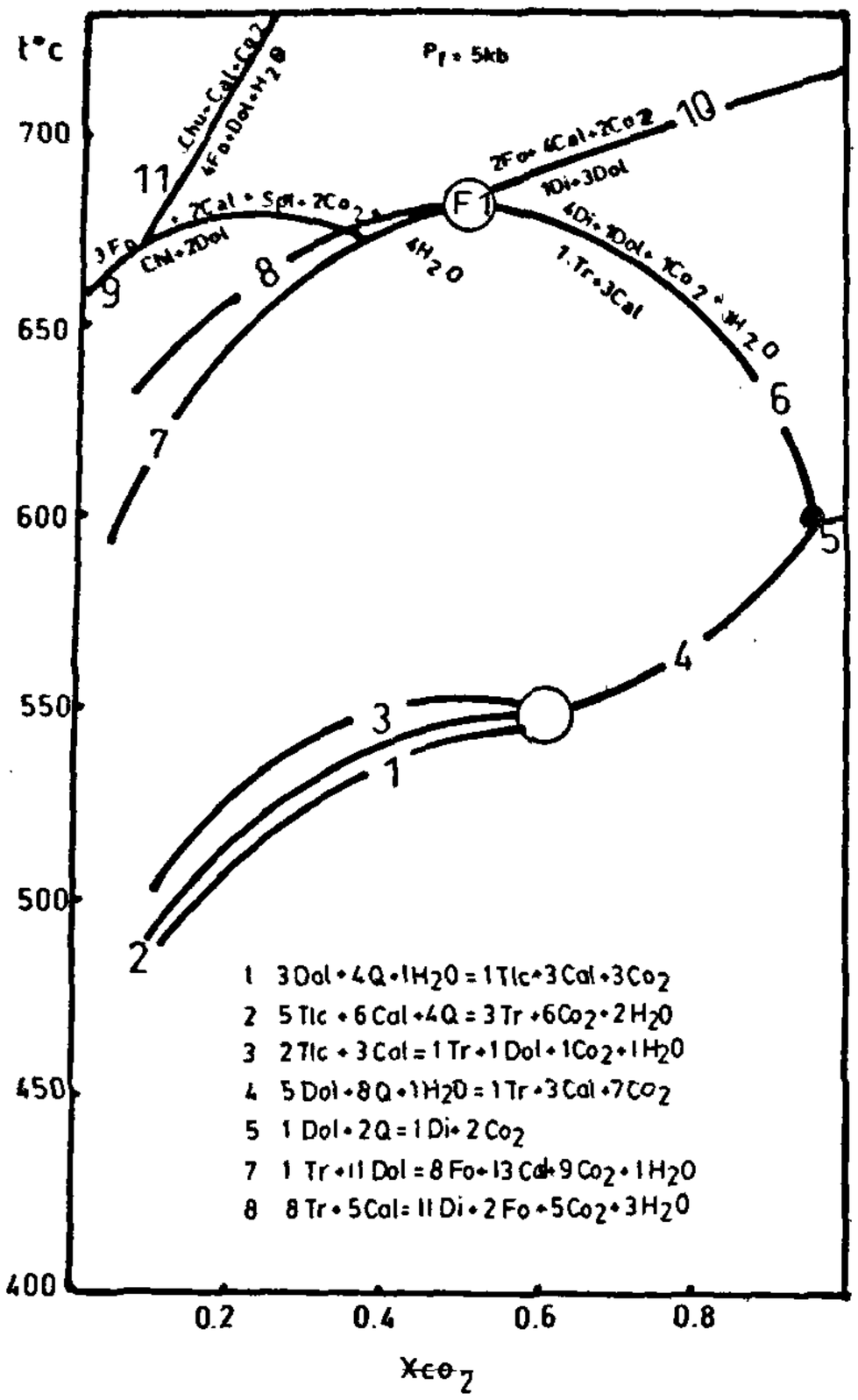

Figure 3. T–X_{CO_2} diagram for reactions in dolomites (modified after Winkler[28]).

The graphite and sulphides suggest a reducing environment at some locations. The modal proportions of the minerals in the whole rock analysed average humite 28.5 + spinel 13.7 + calcite/dolomite 56.2. Exsolved dolomites occur as stringers and blebs in the calcites. Apatite occurs as anhedral crystals (Figure 2). The assemblages talc + tremolite + calcite + dolomite and talc + calcite + dolomite represent the last stages of retrogression.

Methodology

Trace and REE contents of marble rocks, the separated apatite, calcite/dolomite, spinel and humite were determined using a Plasma Quad PQI Inductively Coupled Plasma-Mass Spectrometer (ICP-MS) at the National Geophysical Research Institute (NGRI), Hyderabad. The major elements were determined using a Wavelength Dispersive System Camebax EPMA also at NGRI. The operational and analytical procedures of both are available elsewhere[12–14]. The chondrite normalization values used are that of Nakamura[15] with additions from Haskin *et al.*[16].

REE in metamorphic rocks

Only rarely have studies been attempted on trace and REE residences in individual minerals of metamorphic rocks. To date, there are no published trace and REE data on humites. REE content in metamorphic rocks has been used to determine the nature of the Archaean crust or to study deep crustal processes[17,18]. Under closed systems, the protolith REE is preserved in its metamorphic equivalent[19].

There is limited major element variation among the analysed humites, spinel and calcite/dolomite. The elemental distribution between mineral phases is systematic and equilibrium conditions may have been achieved. The major, trace and REE chemistry of the analysed minerals and the whole rock samples are presented in Tables 1a and b.

Major element chemistry

Humite. A notable feature of the mineral assemblages of Ambasamudram is the abundant occurrence of humites, which are stable only in F-rich aqueous fluids, with low X_{CO_2}. The stability field of the humites and the associated phases are shown in the *T–X* diagram (Figure 3). The TiO_2 contents are below 1.00 weight per cent, typical of marbles. The Mg/Mg+Fe ratio (X_{mg}) is greater than 0.98, indicating limited Fe–Mg substitution.

Calcite. Calcite grains contain exsolved patches of dolomite, FeO and MnO are less than 0.2 weight per cent. Sr is 116 ppm.

Spinel. The spinels are magnesium aluminate spinels with minor hercynite content (X_{mg} = 0.96). FeO is preferentially accommodated in spinels and FeO weight percentage averages 2.36. The Al_2O_3 content is 70.81 and MgO 27.74.

Tremolite. The amphibole has been classified as tremolite based on Leake's classification[20] with X_{mg} value >0.98. The CaO content of 13.74 is typical of tremolites in sedimentary marbles.

Apatite. Apatite is present in minor amounts. The average CaO weight percentage is 56.4, P_2O_5 is 42.01. 0.01 weight per cent MnO and 0.02 weight per cent TiO_2 are also found. Coupled substitution of Si^{4+} for P^{5+} and Na^{+} for Ca^{2+} may have occurred in the apatites, during REE fractionation.

Table 1a. Major† and trace‡ element contents of the minerals and marble

Wt%	Chondrodite	Calcite	Spinel	Apatite	Marble*	Tremolite
SiO_2	34.28	0.00	0.02	0.00	10.29	54.00
TiO_2	0.59	0.05	0.03	0.02	0.21	0.18
Al_2O_3	0.01	0.06	70.81	0.00	10.66	4.47
FeO	1.70	0.12	2.36	0.01	0.93	0.30
MnO	0.19	0.14	0.09	0.02	0.15	0.08
MgO	61.57	4.26	27.74	0.01	24.98	25.95
CaO	0.08	51.85	0.05	56.40	28.60	13.34
Na_2O	0.04	0.00	0.00	0.00	0.01	0.11
K_2O	0.03	0.02	0.03	0.00	0.03	0.03
P_2O_5				42.01	0.04	
ppm						
Sc	1.83	1.18	0.86	0.67	1.76	
V	61.34	18.09	1218.36	25.81	32.69	
Cr	4.44	4.52	111.15	7.66	6.42	
Co	6.25	1.03	6.69	0.89	2.22	
Ni	50.62	9.54	24.90	22.57	23.82	na
Cu	4.82	4.43	94.30	126.32	3.87	
Zn	28.95	5.97	510.07	25.46	25.91	
Ga	0.01	0.13	24.19	0.68	0.97	
Rb	0.05	0.01	0.24	0.59	0.01	
Sr	5.96	115.99	9.01	334.05	101.44	
Y	1.95	7.88	3.86	26.94	7.32	
Zr	34.79	8.87	78.77	29.79	43.23	
Nb	2.93	bd	0.14	0.32	0.86	
Cs	bd	bd	0.03	0.06	bd	
Ba	39.47	28.87	27.52	24.41	32.19	
Hf	1.10	0.31	2.10	0.37	1.14	
Ta	0.33	bd	0.09	0.22	0.03	
Pb	1.87	2.05	4.46	7.83	1.54	
Th	0.31	0.35	0.31	51.95	0.47	
U	0.04	0.06	0.16	49.23	0.03	

bd, below detection; +, Using EPMA; ‡, Using ICP-MS; na, not analysed; * Based on modal mineralogy.

Table 1b. REE‡ content of minerals and marble (in ppm)

Wt%	Humite	Calcite	Spinel	Apatite	Marble
La	0.62	5.25	0.94	29.65	15.00
Ce	0.46	7.75	0.78	55.59	24.00
Pr	0.06	0.95	0.06	6.20	2.64
Nd	0.31	3.78	0.43	26.06	11.74
Sm	bd	0.59	bd	5.05	3.33
Eu	0.03	0.21	0.05	1.05	0.48
Gd	0.04	0.95	0.08	5.05	2.00
Tb	0.01	0.12	0.01	0.65	0.14
Dy	0.02	1.02	0.03	3.78	2.24
Ho	bd	0.17	bd	0.63	0.39
Er	bd	0.59	bd	1.51	1.09
Tm	bd	0.06	bd	0.21	0.10
Yb	bd	0.47	bd	1.28	0.66
Lu	0.01	0.06	bd	0.12	0.08
REE	1.56	21.97	2.38	136.84	63.89
La/Sm	68.08[a]	8.89	104.44[a]	5.87	4.50
Gd/Yb	4.40[b]	2.02	8.88[b]	3.94	3.03
[c]Eu/Eb*	–	0.86	–	0.65	0.62

bd, below detection; a, assuming Sm = 0.009; b, assuming Yb = 0.009; c, $Eu/Eu^* = Eu(N)/\sqrt{Sm(N) \times Gd(N)}$ where N denotes normalized value; +, Using EPMA; ‡, using ICP-MS; na, not analysed.

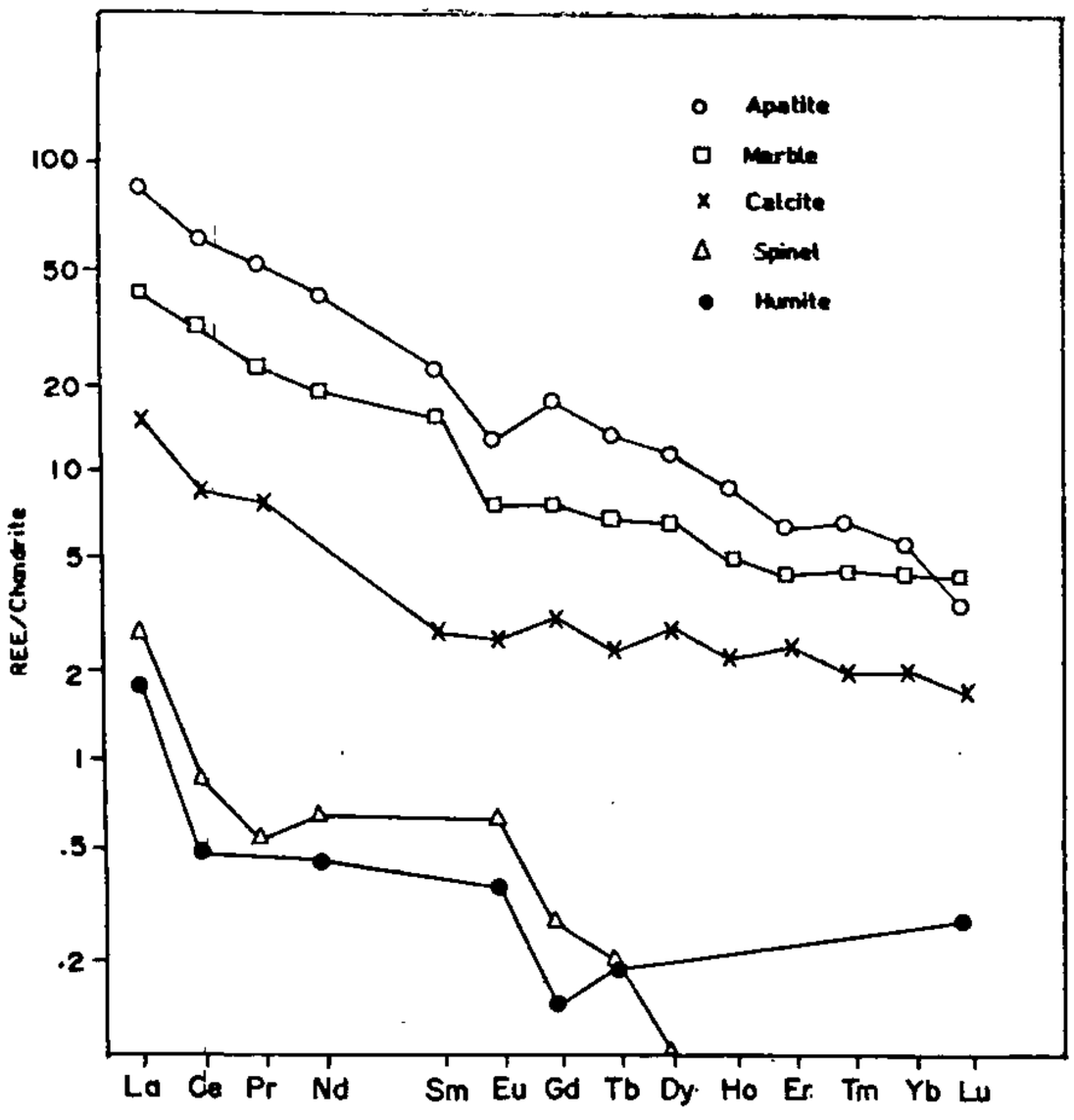

Figure 4. Chondrite-normalized REE patterns (Masuda–Coryell diagram) of Ambasamudram marbles and minerals.

REE residence in individual minerals

Apatite. Chondrite-normalized Masuda-Coryell diagrams of the analysed apatites (Figure 4) exhibit a maximum at La and a minimum at Lu. The absolute concentrations are forty times chondrite. All apatites show negative europium anomalies. Apatites usually contain about 0.1 weight per cent REE. This replaces Ca in the structure. The Ambasamudram apatites are enriched in light REEs (La/Sm = 5.87) relative to heavy REEs (Gd/Yb = 3.94). La is the dominant lanthanide. Co and Er show small negative variation from the trend of lanthanide distribution. Apatites contain the highest concentration of REEs among the analysed minerals. The higher La/Sm ratio indicates the strong LREE fractionation into apatite.

Calcite. Calcite grains exhibit a maximum at La and a minimum at Lu. The LREE (La/Sm = 8.89) are enriched relative to HREE (Gd/Yb = 2.02). The average total REE content in the calcite grain is 21.97 ppm, nearly six times chondrite. There is a small negative europium anomaly, with average Eu/Eu* ratio of 0.86. Ce, Tb and Ho show negative anomalies. The calcites have the second highest concentration of REE among the analysed minerals in the marbles. The REEs substitute for Ca in the calcite grains. This is due to the similarity in ionic radii of calcite (1.08 Å) and REEs (0.97–1.14 Å). The higher La/Sm ratio indicates LREE enrichment in calcites.

Humite. Humites exhibit a maximum at La. Many of the LREEs (Pm, Sm) and HREEs (Dy, Ho, Er, Tm, Yb) are below 0.01 ppm, the detection limit of the ICP-MS. Among the detected elements, the minima is at Gd. The humites also exhibit a negative Ce anomaly. There is a positive Eu anomaly in the humite pattern but this is not a dependable estimate since Sm was below detection limits. LREEs (La/Sm = 68.8) are enriched relative to the HREEs (Gd/Yb = 4.4).

Spinel. Spinels exhibit a maximum at La and minimum at Dy. There is a marked negative Pr anomaly. The LREEs (La/Sm = 104.44) are enriched relative to the HREEs (Gd/Yb = 8.88). The LREEs (Pm and Sm) and HREEs (Ho, Er, Tm, Yb and Lu) are below detection limits.

Marbles. The most abundant lanthanide in the marbles is cerium. The rocks have a negative europium anomaly of 0.76. The LREE is relatively enriched and the HREE pattern is nearly flat. The La/Sm value is 4.5 and Gd/Yb is 3.03. Ho, Tm, Lu are near the detection limits of the ICP-MS.

Zr is the only trace element distributed nearly uniformly in all the four mineral phases and the rock. Zr would have been mobilized by the fluids and incorporated into the minerals. Sr is the most abundant trace element in calcite (115.99 ppm), apatite (334.05 ppm) and marble (101.44 ppm) while in both humite and spinel vanadium is the most abundant (61.44 ppm and 1218.36 ppm respectively). Ba is also abundant in all the phases and ranges from 24.41 ppm in apatite to 39.47 ppm in humites. It can be summarized that Zr, Sr, V, Zn, Ba, Cu, Ni and Co are the most abundant trace elements in these phases. Apatite contains 51.95 ppm Th and 49.23 ppm U. In humites V, Ni, Ba, Zr, Zn, Ca, Sr, Cu, Cr, Nb, Y, Pb, Sc, Hf, Ta, Th, Rb, U and Ga occur in order of decreasing abundance.

Relation between REE and major element content

The most abundant major elements in all the analysed minerals are Mg ± Ca ± Si ± Al. Besides these, apatite contains 5 atoms per formula unit (apfu) P and humites about 0.03 apfu Ti. The stoichiometric proportions of the major elements have been normalized to 100 anions (Table 2) and designated by the subscript *n*. On this basis the apatites contain the maximum normalized Ca value, $Ca_n = 38.6$, whereas calcite has $Ca_n = 32.7$. The highest Mg_n is in humite (49.44), next in abundance is in spinel (24.68), calcite (0.33) and apatite (0.019). Spinels, calcites and apatites have no Si_n. Calcite and apatite have no Al_n whereas it is low in humite (0.003). Spinel has the highest Al_n of 48.00. Though the calcite grains and apatites have close Ca_n (38.6 and 32.7 respectively), their REE contents differ markedly (21.97 ppm and 136.84 ppm respectively). The apatites are relatively late stage minerals. The fluids mobilize REE from pre-existing hosts and concentrates them into minerals such as apatites. High concentration of P_n (23.08) in apatite is also a major factor in REE concentration. Calcites with exsolved dolomites and dolomites *per se* are quite abundant in the Ambasamudram marbles but are megascopically indistinguishable. Higher the dolomite content higher will be the Mg_n, thus restricting REE fractionation into the carbonate minerals. The analysed minerals are arranged in Figure 5 in increasing order of Ca_n along the *X*-axis (not to scale) and total REE plotted against each along the *Y*-axis. It is obvious that both LREE and HREE are preferentially accommodated in Ca and/or P-rich, Mg–Al–Si-poor phases. There is a strong correlation between the Ca and/or P content and REE enrichment. Si^{4+} is an inhibiting factor in REE concentration, because of its incompatible valency of 4+ and ionic radius of 0.34 Å. Mg too has a similar but less drastic effect. The Mg ionic radius (0.80 Å) is closer to that of the REEs (0.97–1.14 Å), than that of Si. Al has a

Table 2. Normalized cation contents, cation radii and total REE in the analysed minerals

	Cations/100 anions and ionic radii					
Mineral	Ca_n (1.08 Å)	Mg_n (0.80 Å)	Si_n (0.34 Å)	Al_n (0.61 Å)	P_n (0.91 Å)	Total REE (in ppm) (0.97–1.14 Å)
Apatite $Ca_5(PO_4)_3(OH, F)$	38.60	0.02	0.00	0.00	23.08	136.84
Calcite/dolomite $CaCO_3/CaMg(CO_3)_2$	25.14	8.13	0.00	0.00	0.00	21.97
Humite n $Mg_2SiO_4 \cdot Mg(OH, F)_2$	0.03	49.44	22.20	0.00	0.00	1.56
Spinel $Mg\ Al_2O_4$	0.03	24.68	0.00	48.00	0.00	2.38

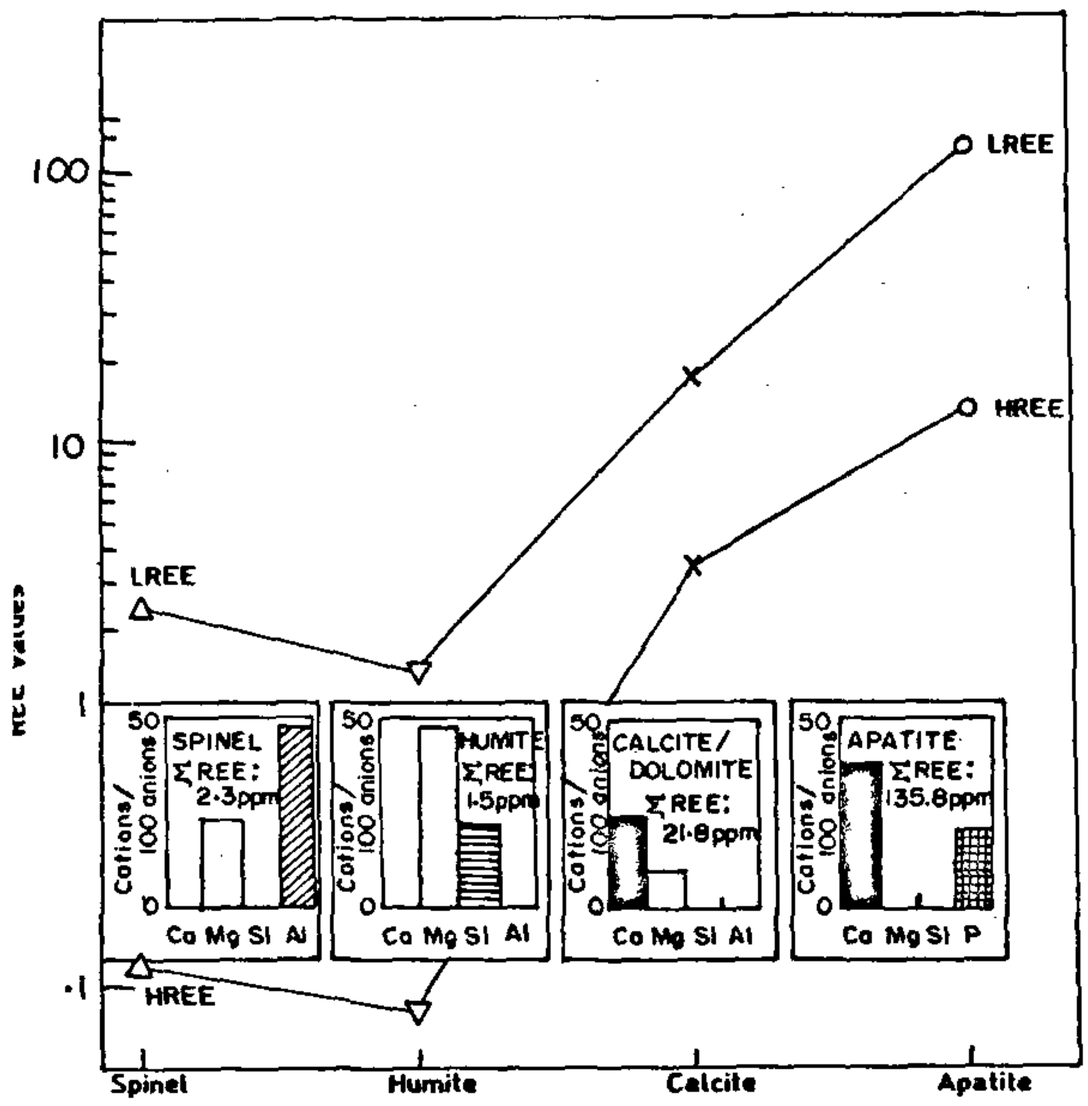

Figure 5. REE abundances of spinel, humite, calcite/dolomite and apatite plotted against the respective mineral. Each inset shows the Ca_n, Mg_n, Si_n and Al_n values. In apatite instead of Al_n, P_n is shown. The relation between major element type and abundance to the REE abundance is evident.

charge of 3+, but the ionic radius is only 0.61 Å, thus discounting REE fractionation into Al-sites. The role of P in REE distribution in the minerals and rocks analysed is in conformity with earlier studies[21]. The trend of REE enrichment of the minerals and rocks analysed with respect to their normalized major element content is shown in Table 3.

REE enrichment in apatite

Apatites with their open structure and high Ca and P contents preferentially accommodate REEs. In igneous melts, apatites are one of the last minerals to crystallize and REEs get concentrated in them; but in metamorphic rocks with complex deformational history and episodes of crystal growth/non-growth and fluid activity, such a simplified model is not really applicable. It is proposed that the REEs have been concentrated in apatites because of the following reasons:

1. Availability of two Ca sites, Ca1 and Ca2. The Ca1 site has nine-fold coordination with O atoms, while the Ca2 is coordinated by six O atoms and OH or F. The Mn, Mg, Ti and most of the trace and REE elements substitute for Ca in these sites.

2. Availability of a mechanism for coupled substitution of Na^+ for Ca^{2+} and Si^{4+} for P^{5+} when the trivalent REEs substitute for divalent Ca.

Table 3. Trend of REE abundance with respect to Ca_n, P_n, Mg_n, Si_n and Al_n

	Order of abundance
LREE	Apatite > calcite > spinel > humite
HREE	Apatite > calcite > spinel > humite
REE	Apatite > calcite > spinel > humite
Ca_n	Apatite > calcite >> spinel = humite
P_n	Apatite >> calcite = spinel = humite = 0
Mg_n	Apatite < calcite << spinel < humite
Si_n	Apatite = calcite = spinel = 0<< humite
Al_n	Apatite = calcite = humite = 0 << spinel

3. The surface structures which are conducive to the differential partitioning of trace and REE into apatite. The role of these surfaces has been brought out by the occurrence of sectoral and intrasectoral zoning in apatite[22].

4. Apatites, which are anhedral, formed in the last stages of metamorphism, after the formation of humites. The humites have accommodated the bulk of the fluorine. The REEs have been mobilized from host rocks by F-rich aqueous fluid activity coinciding with the formation of granitic gneisses found closely associated with the marbles and fixed in the minerals during retrogression. Apatites have preferentially accommodated the REEs.

This strongly suggests the influence of fluid activity on the REE fractionation and movement in marbles and related rocks. The negative Eu anomaly in apatites, calcites and the rock indicate low oxygen fugacities, and under such conditions Eu^{2+} is not taken into their structures[23]. The high Ce content in apatites indicates that the original sedimentary material had also a high Ce value. No metamorphosed equivalents of Mn-nodules, which preferentially accommodate[24] Ce, have been found. This possibly led to the Ce being taken up in apatite. Mn-nodules are absent in shallow shelf waters and the Ce content in apatite indirectly indicates that the Ambasamudram marbles were initially deposited as shallow water shelf facies impure carbonates.

Partitioning of REE

The partition coefficients (Kd.s) of REEs for the mineral assemblages have been calculated and shown in Table 4. These values have been plotted with respect to each element in Figure 6. Apatite and calcite selectively concentrate the REEs in the marbles much more than humite or spinel. This is because REEs have a greater affinity for Ca, and P provides a charge balancing mechanism.

Apatite usually contains 0.1 weight per cent REE. The Ambai apatites contain 0.137 weight per cent REE. In calcites REEs replace Ca^{2+} ions. Partitioning of REEs into apatite relative to humite and spinel is much more

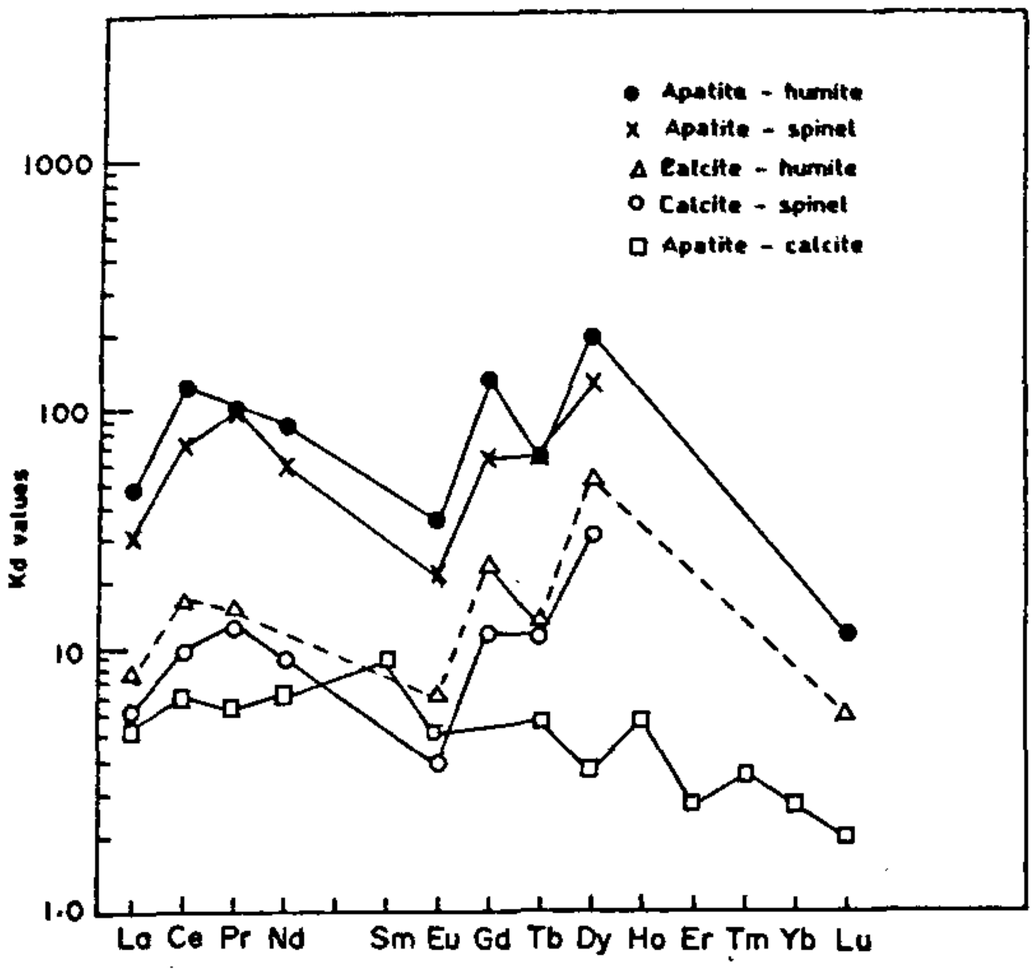

Figure 6. Distribution coefficient of each lanthanide, between mineral pairs, plotted against that particular lanthanide.

Table 4. Partition coefficients (Kd)* of each lanthanide for different mineral pairs

REE	Apatite–calcite	Apatite–humite	Apatite–spinel	Calcite–humite	Calcite–spinel	Humite–spinel
La	5.65	47.82	31.51	8.47	5.59	0.66
Ce	7.17	121.26	71.41	16.85	9.94	0.59
Pr	6.53	102.51	103.33	15.83	15.83	1.00
Nd	6.89	84.06	60.60	12.19	8.79	0.72
Sm	8.56	–	–	–	–	–
Eu	5.05	35.33	21.20	7.00	4.20	0.60
Gd	5.32	126.25	63.13	23.75	11.88	0.50
Tb	5.42	65.00	65.00	12.00	12.00	1.00
Dy	3.71	189.00	126.00	51.00	34.00	0.67
Ho	5.88	–	–	–	–	–
Er	2.56	–	–	–	–	–
Tm	3.50	–	–	–	–	–
Yb	2.72	–	–	–	–	–
Lu	2.00	12.00	–	6.00	–	–

*Kd, concentration of element 1 in mineral A/Concentration of element 1 in mineral B.

marked than that of apatite relative to calcite. There is strong partitioning of Ce, Gd and Dy relative to spinel in apatite, and Ce, Pr, Gd and Dy relative to humite in apatite. The partitioning of LREE into apatite relative to calcite is more efficient than that of HREE. Compared to other REEs, La, Eu and Tb are partitioned less efficiently into apatite and calcite relative to humite and spinel. Except for Pr and Tb, spinels are more enriched in REEs than humites. Also, the LREEs are more effectively partitioned into humites.

Inferences from the trace and REE contents

The total REE contents of the marbles are similar to those reported elsewhere[25] and is very much less than the 10^3–10^4 ppm range for carbonatites and thus indicate that the marbles have no carbonatitic affinity (Table 5 and Figure 7). The REE content is above the average for a limestone[26] and remobilized REE constitutes a major part of it. The negative Eu and Ce anomalies, the flat HREE pattern, and coronitic replacement textures around forsterites further prove the nature of the marbles. Geochemically, the low TiO_2 values of humites (<1.0 weight per cent, Table 6) and low Sr content in apatites (115.99 ppm) are in contrast to the higher values in carbonatites ($TiO_2 > 2.5$ weight percentage, Sr > 7000 ppm). The anhedral apatites are in contrast to the euhedral or ovoid apatites in carbonatites.

Table 5. Comparative REE contents of marbles and carbonatites (in ppm)

	1	2	3	4	5	6
La	15.00	14.38	5.5	<20	1.98	608.0
Ce	24.00	22.32	23.3	<15	5.62	1687.0
Pr	2.64	3.08	2.2		0.57	219.0
Nd	11.74	11.24	9.4	<25	2.26	883.0
Sm	3.33	2.16	2.6		0.79	130.0
Eu	0.48	0.47	0.4		0.76	39.0
Gd	2.00	1.79	2.6			105.0
Tb	0.14	0.00	0.4		0.10	9.0
Dy	2.24	1.46	1.8		0.38	34.0
Ho	0.39	0.30	0.6		0.08	6.0
Er	1.09	0.90	1.0		0.28	0.0
Tm	0.10	0.00			0.03	1.0
Yb	0.66	0.70	1.0		0.19	5.0
Lu	0.08	0.10	0.4		0.03	0.7
ΣREE	63.89	58.90	51.3	<60	13.07	3726.7

1, Ambasamudram marbles; 2, Vinjamur marbles[25]; 3, Average limestone[26] (carbonate rock and deep sea carbonate); 4, Bergell dolomitic marble[1]; 5, Clinohumite–spinel zone, Bergell dolomitic marble[1]; 6, Carbonatites[31].

Table 6. Major element chemistry of humites from marbles and carbonatites

	1	2
SiO_2	34.28	38.12
TiO_2	0.59	3.10
Al_2O_3	0.01	0.00
FeO	1.70	3.99
MnO	0.19	0.51
MgO	61.57	53.52
CaO	0.08	0.00
Na_2O	0.04	0.08
K_2O	0.03	–
Total	98.49	99.32

1. Chondrodite, Ambasamudram marbles, India
2. Titanian clinohumite, Jacupiranga carbonatites, Brazil[32].

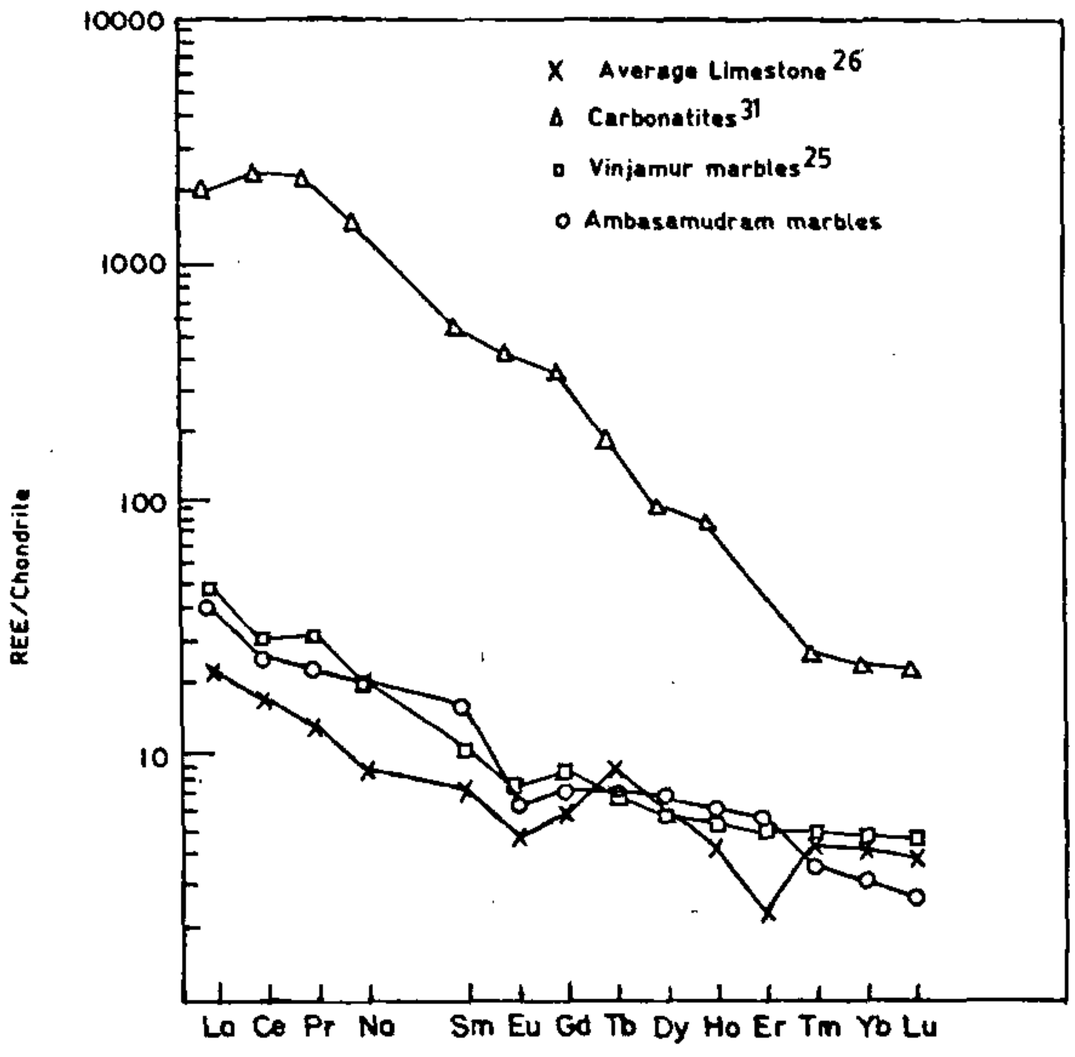

Figure 7. Chondrite normalized REE diagram (Masuda–Coryell diagram) of REE abundance in limestone, carbonatites and marbles.

The fluids

The presence of humites and apatites in the marbles indicates the influx of aqueous F-rich fluids. Humites form only in the presence of H_2O-rich fluids at a finite partial pressure[27] of F (Figure 3). The presence of wollastonite indicates that the system was depleted in CO_2 fluids. However the isolated patches of calc-silicates containing scapolites indicate a relatively closed/open nature of the system, with differing CO_2 levels, consequent upon the structural controls associated with a ductile shear zone like the ASZ.

During high grade metamorphism X_{CO_2} may have reached relatively high values. The high grade reactions like 7 and 8 occur over a range of X_{CO_2} values (<0.1–0.5) with increasing temperatures[28]. The invariant assemblage Fo + Tr + Di + Cal + Dol indicates that at 5 kb and 675°C the X_{CO_2} value[28] was at least 0.5. Forsterite and diopside forming reactions occurred under relatively closed system conditions, with increasing X_{CO_2}.

The stability field for clinohumite + calcite is restricted to fluids with $X_{CO_2} = 0.40$ at temperatures greater[29] than 550°C. The occurrence of the clinohumite-bearing assemblages thus indicates the H_2O-rich nature of the fluids. Thus an influx of aqueous fluorinated fluids is essential for humite formation and most of the retrograde reactions involve decreasing CO_2 contents, the fluids being progressively diluted by the H_2O-rich fluids. Fluids generated from igneous intrusions are capable of having a fluid–rock ratio in excess of two[30]. The abundance of humites in these rocks and the presence of F in most of the hydrous minerals would require such large influxes. The marbles were, thus, initially in a high CO_2 environment.

The shearing and the associated granite emplacement triggered the movement of the aqueous fluorinated REE-bearing granitic fluids, which in turn brought about the formation of the humites and triggered REE movement and incorporation. This shearing occurred along the ASZ before the metamorphic peak was reached. Forsterite started conversion to clinohumite and chondrodite as also tremolite to clinohumite at the temperature peak. Retrogression had set in thereafter, but even then the marbles were responding to the high temperature and the continuing fluorine activity prompted the formation of the F-rich humite minerals. With dropping temperatures, tremolite and talc were the last phases to develop.

The extremely F-rich nature of the fluids led to the effective complexing and mobilization of the REEs. F-rich hydrothermal fluids are capable of transporting REEs[3]. These fluids, probably at temperatures greater than 650°C, will complex REEs, yielding fluoride–REE complexes. It has been found that most REE in acidic solutions rich in F occurs as RE $(Cl, F)_2^+$. The presence of F significantly increases REE mobility, Go values become more strongly negative for solution reactions, yielding (RE) F_2^+ and La $(RE)F_3$ (ref. 4). With increasing temperatures the F-rich REE-bearing fluids mobilized additional REEs from pre-existing high grade hosts. Subsequently during retrogression, with decreasing fluid temperatures the REEs were progressively incorporated into the structure of calcite/dolomite and apatite and the activity of the fluid continued till talc was formed.

The REE concentration in minerals during high grade metamorphism was probably low since most reactions took place in a high X_{CO_2} condition. Whatever REEs that resided in the high grade assemblages were flushed out by the fluid activity. The F-rich aqueous fluid is a bus for Ti, Zr and the REEs. Some Ti in these fluids have been incorporated in the humites, but the majority has been accommodated in rutile and ilmenite, phases present in minor amounts.

Summary and conclusions

The crystal structure and chemistry of a mineral, the charge, the ionic radii and coordination of the elements and their relative abundance are the most important factors in the concentration of REEs. Most REEs reside in calcites in the widespread humite–calcite–spinel assemblage in the marbles, though apatites are the most REE-rich of all the minerals. The field, mineralogical, and geochemical data unequivocally prove the sedimentary parentage of the Ambasamudram marbles. These were originally shallow-water shelf-facies impure carbonate sediments. Zr, Ti and REEs are quite mobile in

the conditions available in the area. During high grade conditions, the REE content in the marbles was low. The REEs have been mobilized by the fluorinated aqueous fluids associated with the granites and granitoids, as late stage residual granitic fluids and fixed in the mineral structure of apatite and calcite during the retrograde metamorphism into amphibolite-upper greenschist facies, in a relatively open system with low X_{CO_2}. The source of the REE fluids at Ambasamudram is thus external to the marbles.

The fluid–rock ratios are currently being investigated, as also stable isotope ratios for indications of alternate sources. The study of the vein mineralogy, chemistry and attendant fluid and REE activities in areas of humite occurrences could provide models for predicting the effects of halogen-rich fluids on geological materials used as hazardous waste repositories. The temporal extent of the REE mobilization and incorporation coincided with the period over which the halogenated aqueous fluid was active.

1. Ried, F. A., Ph D thesis, ETH, Zurich, 1994, p. 204.
2. Giere, R., Ph D thesis, ETH, Zurich, 1990, p. 250.
3. Wood, S. A., *Chem. Geol.*, 1990, **88**, 99–125.
4. Humphris, S. E., in *Rare Earth Element Geochemistry. Developments in Geochemistry* (ed. Henderson, P.), Elsevier, Amsterdam, 1984, vol. 2, pp. 317–342.
5. Krishnanath, R., *J. Geol. Soc. India*, 1981, **22**, 235–242.
6. Pradeepkumar, A. P. and Krishnanath, R., 1996 (MS in preparation).
7. Drury, S. A., Harris, N. B. W., Holt, R. W. and Reeves-Smith, G. J., *J. Geol.*, 1984, **92**, 3–20.
8. Windley, B. F., Razafiniparany, A., Razakamanana, T. and Ackermand, D., *Geol. Rundsch.*, 1994, **83**, 642–659.
9. Nicollet, C., in *Granulites and Crustal Evolution* (eds Vielzuf, D. and Vidal, Ph.), Kluwer, Dodrecht, 1990, pp. 291–310.
10. Kriegsman, L. M., *Precam. Res.*, 1995, **75**, 263–277.
11. Pradeepkumar, A. P., Rosen, K., Krishnanath, R. and Raith, M., (abstract) V. M. Goldschmidt International Geochemistry Conference, Heidelberg, 1996.
12. Balaram, V., *J. Indian Chem. Soc.*, 1991, **68**, 600–603.
13. Balaram, V., *Curr. Sci.*, 1995, **69**, 640–649.
14. Lifshin, E., in *Materials Science and Technology: A Comprehensive Treatment* (ed. Lifshin, E.), VCH Verlagsgesellschaft mbH, Weinheim, 1994, vol. 2, pp. 352–421.
15. Nakamura, N., *Geochim. Cosmochim. Acta*, 1974, **38**, 757–775.
16. Haskin, L. A., Haskin, M. A., Frey, F. A. and Wildeman, T. R., in *Origin and Distribution of the Elements* (ed. Ahrens, L. H.), Pergamon, Oxford, 1968, vol. 1, pp. 889–911.
17. Newton, R. C., *J. Met. Geol.*, 1992, **10**, 383–400.
18. Newton, R. C., *Eur. J. Min.*, 1995, **7**, 861–881.
19. Grauch, R. I., in *Geochemistry and Mineralogy of Rare Earth Elements. Reviews in Mineralogy* (eds. Lipin, B. R. and McKay, G. A.), Mineralogical Society of America, Washington DC, 1989, vol. 21, pp. 149–167.
20. Leake, B. E., *Min. Mag.*, 1978, **42**, 533–565.
21. Ryerson, F. J. and Hess, P. C., *Geochim. Cosmochim. Acta*, 1980, **44**, 611–624.
22. Rakovan, J. and Reeder, R. J., *Am. Min.*, 1994, **79**, 892–903.
23. Puchelt, H. and Emmermann, R., *Earth Planet. Sci. Lett.*, 1976, **31**, 279–286.
24. Elderfield, H., Hawkesworth, C. J., Greaves, M. J. and Calvert, S. E., *Geochim. Cosmochim. Acta*, 1981, **45**, 513–528.
25. Subbarao, K. V., Lebas, M. J. and Bhaskar Rao, B., *J. Geol. Soc. India*, 1995, **46**, 125–137.
26. Turekian, K. K. and Wedepohl, K. H., *Bull. Geol. Soc. Am.*, 1961, **72**, 175–192.
27. Bucher, K. and Frey, M., *Petrogenesis of Metamorphic Rocks*, Springer, Berlin, 1994, 6th edn, p. 318.
28. Winkler, H. G. F., *Petrogenesis of Metamorphic Rocks*, Springer, New York, 1979, 5th edn, p. 348.
29. Rice, J. M., *Contrib. Mineral. Petrol.*, 1980, **71**, 219–235.
30. Ferry, J. M., *J. Geol. Soc. London*, 1983, **140**, 551–556.
31. Woolley, A. R. and Kempe, D. R. C., in *Carbonatites–Genesis and Evolution* (ed. Bell, K.), Unwin Hyman, London, 1989, pp. 1–14.
32. Gaspar, J. C., *Am. Min.*, 1992, **77**, 168–178.

ACKNOWLEDGEMENTS. We thank Mr R. Natarajan, NGRI, for the EPMA results and Dr V. Balaram, NGRI, for the ICP-MS analyses. A.P.P. thanks the UGC for awarding SRF. This work forms part of his Ph D thesis on the humite marbles of Ambasamudram. We thank the referee for useful suggestions which have improved the quality of the paper.

Received 4 January 1996; revised accepted 2 May 1996